RESEARCH PAPER

Synthesis, Characterization, and Antiproliferative Evaluation of a Quinazoline-Based Compound Against A549 Non-Small-Cell Lung Carcinoma.

Srinivasan.M[1], Ismail.Y[1]*

[1]Research Scholar, Crescent School of Pharmacy, B.S. Abdur Rahman Crescent Institute of Science & Technology, Vandalur, Chennai-600048, Tamilnadu, India.
[1].Professor, Crescent School of Pharmacy, B.S. Abdur Rahman Crescent Institute of Science & Technology, Vandalur, Chennai-600048,Tamilnadu, India.*

ABSTRACT
A novel quinazoline-based compound, 4-(1-(2-amino-6,7-dimethoxyquinazolin-4-yl)-1,4- dihydropyridin-3-yl)methylbenzoic acid, was synthesized and characterized as a potential therapeutic agent targeting non-small-cell lung carcinoma (NSCLC) cells. The compound was prepared via a two-step synthetic process—alkylation followed by condensation—and its structure was confirmed through infrared (IR), nuclear magnetic resonance (NMR), mass spectrometry, and X-ray diffraction analyses. To evaluate its antiproliferative efficacy, a concentration-dependent cytotoxicity assay (MTT) was conducted using A549 human NSCLC cells. The compound exhibited strong cytotoxic potential with a calculated IC value of 19.88 µg/mL, alongside significant apoptotic induction confirmed by acridine orange/ethidium bromide (AO/EtBr) dual staining. Morphological assessment under microscopy revealed pronounced apoptotic features that increased in a time-dependent manner, with 57% and 66% apoptotic cells present at 24 and 48 hours, respectively. Molecular docking and induced fit docking studies against the KRAS^G12C protein (PDB: 7AIW) revealed high-affinity binding, stabilized by a network of hydrogen bonds and hydrophobic interactions involving critical active-site residues, reflected in a substantial MMGBSA binding energy (−39.25 kcal/mol) and an excellent docking score (−4.47). These findings demonstrate that the synthesized quinazoline derivative possesses promising anticancer activity mediated by apoptosis and strong interactions with oncogenic targets, highlighting its potential as a lead molecule for further mechanistic exploration and drug development against NSCLC.
Keywords: Synthesis Quinazoline derivative, A549 cell line, Cytotoxicity; Apoptosis, Insilico Studies
How to cite this article: Srinivasan M, Ismail Y.; Synthesis, Characterization, and Antiproliferative Evaluation of a Quinazoline-Based Compound Against A549 Non-Small-Cell Lung Carcinoma..Int J Drug Deliv Technol. 2026;16(1s): 303-310; DOI: 10.25258/ijddt.16. 303-310
Source of support: Nil.
Conflict of interest: None

INTRODUCTION

Lung cancer remains the leading cause of cancer-related mortality globally, contributing significantly to the overall cancer burden. Among its subtypes, non-small-cell lung carcinoma (NSCLC) accounts for approximately 85% of all cases, characterized by aggressive proliferation, metastasis, and resistance to standard therapies[1,2]. Despite recent advances in targeted and immunotherapies, the five-year survival rate for advanced NSCLC remains discouragingly low. The persistent challenges of multidrug resistance and systemic toxicity necessitate the continued searchfornoveltherapeuticscaffoldswithselectivecytotoxicityandimprovedpharmacodynamic performance.

Heterocyclic compounds, particularly those based on the quinazoline nucleus, have emergedaspotentpharmacophoresinanticancerdrugdiscovery.Quinazolinederivativesarewell known for their ability to inhibit tyrosine kinases, modulate apoptosis-related pathways, and influence cell cycle arrest[3,4]. Many clinical antineoplastic agents, including gefitinib and erlotinib, owe their efficacy to the inhibitory function of quinazoline cores on the epidermal growth factor receptor (EGFR)[5]. In this context, hybrid quinazoline-based structures incorporating heteroaromatic rings and substituted alkyl chains have shown promising roles in mediating cytotoxic activity through ROS generation, mitochondrial disruption, and kinase pathway modulation[6,7] .

synthesized as a substituted quinazoline derivative, exemplifies this class's structural adaptability and pharmacological potential. Its design integrates a 6,7-dimethoxyquinazoline scaffoldwith a substituted benzoic acid derivative through a piperidyl linkage, providing diverse electronic and hydrophobic interactions conducive to target affinity[8] . Spectroscopic and crystallographic characterizations confirmed the compound’s structure and purity, while computational docking studies predicted its binding properity with kinase targets associated with NSCLC proliferation. Investigating its cytotoxic potential against A549 lung carcinoma cells provides a vital link between the compound’s molecular architecture and biological activity, enabling the assessment of its

**Author for Correspondence:* Dr. Ismail Y.

mechanistic influence on cancer cell viability and apoptosis[9,10]

The KRAS^G12C mutation, a common oncogenic alteration in non-small-cell lung carcinoma (NSCLC), plays a critical role in driving tumor development by continuously activating cell signaling pathways responsible for cell growth and survival. This mutation involves the substitution of glycine with cysteine at position 12 of the KRAS protein, which locks it in an active state, triggering cascades such as MAPK and PI3K that promote uncontrolled proliferation. Representing about 10-15% of NSCLC cases, particularly lung adenocarcinoma, KRAS^G12C mutation is often linked to smoking and distinct co-mutations that influence disease progression and treatment outcomes. The PDB structure 7AIW corresponds to this mutant KRAS in a conformation ideal for molecular docking studies targeting the unique cysteine residue, allowing for selective inhibition efforts. Targeting KRAS^G12C has become a promising therapeutic strategy due to its direct involvement in NSCLC pathogenesis and the availability of novel covalent inhibitors that exploit this mutation, aiming to improve clinical responses in patients resistant to conventional therapies. Selecting the KRAS^G12C PDB 7AIW structure enables precise evaluation of drug binding and interaction dynamics relevant to this aggressive and therapeutically challenging subtype of NSCLC.

This study aimed to (synthesize and characterize through modern spectroscopic methods, evaluateitscytotoxicpotentialintheA549NSCLCcellline,and analyzeitsmechanismofaction throughbiochemicalandmorphologicalassessments.Integrating thesynthetic,spectroscopic,and biological findings presents a comprehensive evaluation of the pharmacological potential of this newlydevelopedquinazolinederivative[11].Despiteadvancesintargetedtherapiesfornon-small- cell lung carcinoma (NSCLC),challenges such as drug resistance and limited efficacy continue to hinder successful treatment outcomes.Quinazoline derivatives have shown substantial promise as anticancer agents, particularly due to their capacity to inhibit kinase-driven pathways involved in tumor growth and survival.Building on this knowledge, the present study focuses on the synthesis and characterization of a novel quinazoline-based compound designed to target NSCLC. We aim to evaluate its cytotoxicity and apoptotic potential in A549 lung carcinoma cells, alongside computational docking studies to elucidate its molecular interactions with relevant protein targets. This integrated approach seeks to provide insights in to the compound's therapeutic feasibility and mechanism of action in NSCLC treatment

Materials and Methodology Chemicals and Reagents

All chemicals and solvents used were of analytical grade and procured from Sigma-Aldrich and Merck. A549NSCLC cells were obtained from the National Centre forCell Science(NCCS, Pune, India). Dulbecco's Modified Eagle Medium (DMEM), fetal bovine serum (FBS), MTT reagent, phosphate-bufferedsaline(PBS),and trypsin-EDTA were purchased from Thermo Fisher Scientific[12].

Experimentalsection

Step1:Alkylationof1,4-dihydropyridinederivative

Asolutionof1,4-dihydropyridine(100mg,0.60mmol)in0.5Mdioxanewastreatedwith 4-(bromomethyl)benzoicacid(76mg,0.63mmol).Thereaction mixturewasrefluxedfor8hours under constant stirring. After the completion of the reaction, confirmed by TLC, distilled water was added, and the mixture was further heated for 2 hours[13]. The organic layer was separated using diethyl ether, dried over anhydrous $MgSO_4$, and the solvent was evaporated under reduced pressure. The crude product was purified by column chromatography using hexane/ethyl acetate (6:1) as eluent to yield the alkylated intermediate.

Step2:Condensationwith4-chloro-6,7-dimethoxyquinazoline

The intermediate was reacted with 4-chloro-6,7-dimethoxyquinazoline (3.14 g, 13.98 mmol) and 3-(4-piperidyl)propanoic acid (2.0 g, 12.72 mmol) in isopropanol (100 mL). The mixture was stirred at 90°C for 3 hours[14]. The reaction mass was evaporated to dryness and triturated with dichloromethane (20 mL).

Characterization

The compound was characterized using IR spectroscopy (PerkinElmerSpectrumIR,4000– 450 cm^{-1}), ^{1}H-NMR and ^{13}C-NMR (400 MHz, DMSO-d_6 solvent), mass spectrometry (ESI-MS, positive mode),[15]and powder X-ray diffraction (Cu Kα source, λ = 1.5418 Å)

CytotoxicityAssay(MTT)

A549 cells were cultured in DMEM supplemented with 10% FBS, 1% penicillin– streptomycin,and incubated at 37°C under 5% CO_2.Cells were seeded at adensityof 1×10^4 cells per well in a 96-well plate and incubated overnight. 4-((1-(2-amino-6,7-dimethoxyquinazolin-4- yl)-1,4-dihydropyridin-3-yl)methyl)benzoic acid was dissolved in DMSO and diluted to final concentrations ranging from5to100µM.After 24h treatment, 10µL of MTT reagent(5mg/mL) was added and incubated for 4 hours[16,17].The formazan crystals were dissolved in DMSO(200 µL/well), and absorbance was measured at 570 nm using a microplate reader. The cell viability percentage was calculated relative to untreated control, and IC_{50} was derived via nonlinear regression.

Morphological Examination

A549 cells treated with 4-((1-(2-amino-6,7-dimethoxyquinazolin-4-yl)-1,4- dihydropyridin-3-yl)methyl)benzoicacid(10and25µM)wereinspectedunderan invertedphase- contrast microscope to observe cellular shrinkage, rounding, and detachment, indicative of apoptotic morphology.

ApoptoticstainingAO/ETBR

The acridine orange/ethidium bromide (AO/EtBr) dual staining technique was performed to identify apoptotic

changes in A549 cells after treatment with the test compounds. Approximately3×10⁴ cellswereseededinsix-wellplatesandincubatedat37°Cinahumidified CO_2atmosphere until they reached 70–80% confluence. The cells were then treated with the IC_{50} concentration of each compound for 24 and 48 hours, while untreated cells served as the control. After the incubation period,the medium was carefully removed,and the wells were washed twice with Dulbecco's phosphate-buffered saline (DPBS) to eliminate non-adherent cells. A staining solution containing acridine orange and ethidium bromide at equal concentrations (100 µg/mL each) was freshly prepared, and 20 µL of this mixture was added to each well[18].The plates were incubated for 30 minutes at room temperature in the dark to avoid photo bleaching, followed by gentle PBS washing to remove excess dye. The cells were immediately examined under a fluorescence microscope fitted with appropriate filters, and images were captured for analysis. Green fluorescent cells were considered viable, yellow to orange cells indicated early apoptosis, and red cells represented late apoptotic or necrotic stages. The proportion of apoptotic cells was quantified by counting stained cells in random microscopic fields and calculating the percentage of apoptotic cells relative to the total number of cells.All procedures were carried out in triplicate to ensure accuracy and reproducibility.

InsilcoStudies

The molecular docking studies were conducted using the KRASG12C protein structure availablefromtheProteinDataBank(PDBID:7AIW).Theprot einwaspreparedinMaestrousing the Protein Preparation Wizard: this involved assignment of bond orders, addition of hydrogens, andoptimizationofhydrogen-bonding networks.Missingside-chainsandloopsweregeneratedas required, and water molecules beyond 5 Å from the binding site were removed to ensure optimal dockingconditions.Thestructurewasthenminimizedusingthe OPLS4forcefieldtorelieveany local strain and optimize geometry. The ligand was designed using a 2D sketch in Maestro and subjected to Lig Prep for generating appropriate ionization states(atpH7.0±2.0),tautomers,and energy minimization via OPLS4. Prior to docking, the receptor grid was generated around the KRASG12C active site, focusing on the region encompassing residue Cys12, Gly13, and the neighboring catalytic pocket. Docking simulations were performed using the Glide XP (Extra Precision) algorithm. Multiple ligandcon formations were sampled,and the best pose based on the lowest docking score was selected for further analysis. The binding free energy of the protein– ligand complex was calculated using the Prime MMGBSA method, with ΔG_bind estimated in vacuum to evaluate the stability and affinity of the interaction. All fixed and flexible receptor/ligand options were properly configured throughout the process to ensure accurate predictions of binding energies and pose selection.
Inducedfit docking

Inducedfitdocking(IFD)was implemented using the Schrodinger Maestrosuite,enabling both receptor and ligand flexibility for enhanced accuracy of binding predictions. The process began with protein structure preparation(PDBID:7AIW),wherehydrogenswereadded, missing side-chains and loops were rebuilt,and protonation states were adjusted.Hydrogenbonds were optimized, and the resulting protein structure was minimized to remove local strain. The ligand was constructed in 2D using Maestro's sketch tool and processed by LigPrep for generation of correct tautomers, ionization states, and conformational sampling at physiological pH. The active site for docking was defined using grid generation centered on the target region of KRASG12C[19]. The IFD protocol was run as follows: first, Glide standard precision (SP) docking was carried out togenerateinitialligandposeswithsoftenedvanderWaalspote ntials.Forthetopcandidateposes, near by proteinside-chains were sampled and refined, allowing them to adjust in response to ligand binding. The protein–ligand complexes were then minimized using the OPLS4 force field. After refinement, the ligand was re-docked into the newly optimized active site using Glide XP (extra precision) docking. The best binding poses were selected according to the XP docking scores. Finally, binding free energies (ΔG_bind) were calculated using the Prime MMGBSA method under vacuum conditions, thus affording a rigorous assessment of the affinity and stability of the ligand–protein interaction after full consideration of induced fit effects[20–22].

RESULT AND DISCUSSION

The synthesis of 4-((1-(2-amino-6,7-dimethoxyquinazolin-4-yl)-1,4-dihydropyridin-3- yl)methyl)benzoic acid was accomplished via a two-step sequence involving alkylation and subsequent condensation reactions. Initially, 1,4-dihydropyridine (100 mg, 0.60 mmol) was subjected to nucleophilic substitution with 4-(bromomethyl)benzoic acid (76 mg, 0.63 mmol) in dioxane(0.5M)underrefluxconditionsfor8hours.Thesubseq uenthydrolysisstepinvolvedthe addition of water and heating for an additional 2 hours to complete the reaction. Isolation of the alkylated intermediate was achieved through extraction with diethyl ether, washing, drying over $MgSO_4$, and concentration under reduced pressure. Purification by column chromatography (hexane/ethyl acetate, 6:1) afforded the intermediate in acceptable yield.

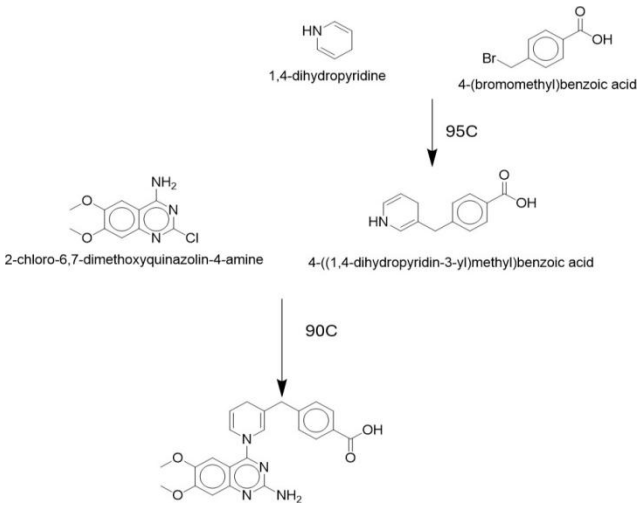

Figure1:Scheme14-((1-(2-amino-6,7-dimethoxyquinazolin-4-yl)-1,4-dihydropyridin-3-yl)methyl)benzoic acid

Inthesecondstep,thepurifiedintermediateunderwentnucleophilicaromaticsubstitution with 4-chloro-6,7-dimethoxyquinazoline(3.14g, 13.98 mmol) and 3-(4-piperidyl)propanoic acid (2.0 g, 12.72 mmol) in isopropanol at 90 °C for 3 hours. Workup involved evaporation and trituration with dichloromethane, yielding 4-((1-(2-amino-6,7-dimethoxyquinazolin-4-yl)-1,4-dihydropyridin-3-yl)methyl)benzoic acid as a white solid in moderate yield (42%)

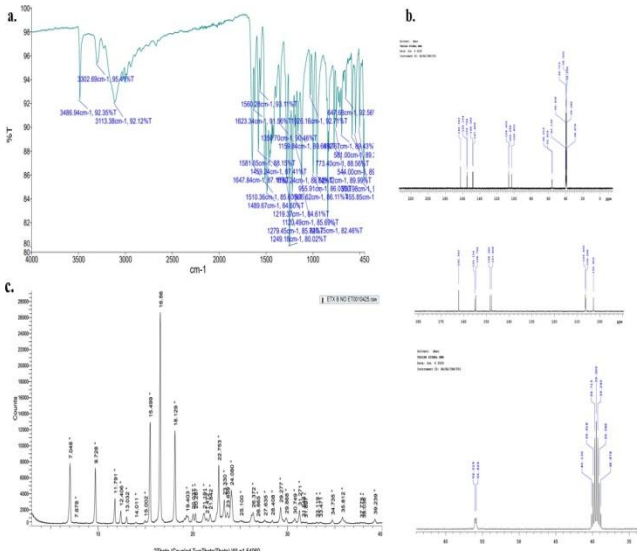

Figure 2 Spectral confirmation of 4-((1-(2-amino-6,7-dimethoxyquinazolin-4-yl)-1,4- dihydropyridin-3-yl)methyl)benzoic acid by IR, NMR and XRD data

the structure of 4-((1-(2-amino-6,7-dimethoxyquinazolin-4-yl)-1,4-dihydropyridin-3-yl)methyl)benzoicacidwaselucidatedviaacombinationofinfrared,nuclearmagneticresonance, and mass spectral analysis as presented. The IR spectrum revealed key absorptions at 3486 cm^{-1} forO–Hstretching,3302cm^{-1}forN–Hstretching,and1648cm^{-1}assignabletocarbonylandimine groups, thus supporting the quinazoline framework. The ^1H NMR spectrum showed aromatic protons spanning δ 7.93–7.06 ppm, methoxy group signals at δ 3.86–3.88 ppm, and aliphatic protonresonancescharacteristicofthedihydropyridinesegmentbetweenδ2.50–3.32ppm.The ^13C NMR spectrum furtherconfirmedthe structurewith resonances for aromaticcarbonsin the δ 162.3–147.8 ppm region and methoxy-substituted carbons near δ 56.0 ppm. Finally, mass spectrometrydisplayedamolecularionpeakatm/z540.39,matchingtheexpectedmolecularmass forthiscompound,thusconclusivelyaffirmingitsidentityitwasFigure2a&bX-raydiffraction (XRD) analysis further confirmed the structural identity and crystallinity of 4-((1-(2-amino-6,7- dimethoxyquinazolin-4-yl)-1,4-dihydropyridin-3-yl)methyl)benzoic acid. The powder XRD spectrum displayed numerous sharp and intense peaks, indicative of a well-defined crystalline phase.Thecharacteristic2θvaluesobservedincluded7.048°,9.728°,11.791°,15.499°(major peak),16.569°,18.129°,22.753°,27.472°,and35.812°,among manyothers.Theoccurrenceand distributionofthesepeaks,withthestrongestreflectionat16.569°,affirmthepresenceofaunique crystalline structure corresponding to the synthesized compound it was depicted on Figure 2c .

The two-step synthetic approach provided are liable route to access the quinazoline-based scaffold with reasonable overall yield and satisfactory purity as evidenced by spectral data. The regioselectivealkylationandsubsequentdisplacementonthechloroquinazolineinthepresenceof the piperidyl acid were achieved under relatively mild conditions, demonstrating synthetic feasibility for the preparation of analogues in future structure-activity relationship studies.

The cytotoxic potential of 4-((1-(2-amino-6,7-dimethoxyquinazolin-4-yl)-1,4- dihydropyridin-3-yl)methyl)benzoic acid was evaluated on the human lung carcinoma A549 cell lineusingtheMTTcolorimetricassay.Thecompoundexhibitedaclear,concentration-dependent inhibitory effect on cell viability. As the concentration increased from 1 µg/mL to 512 µg/mL, a significant reduction in viable cell percentage was observed—from 91.46% at the lowest concentration to 5.49% at the highest. The calculated IC_{50} value was 19.879 µg/mL, indicating substantial cytotoxic potency Figure 3.

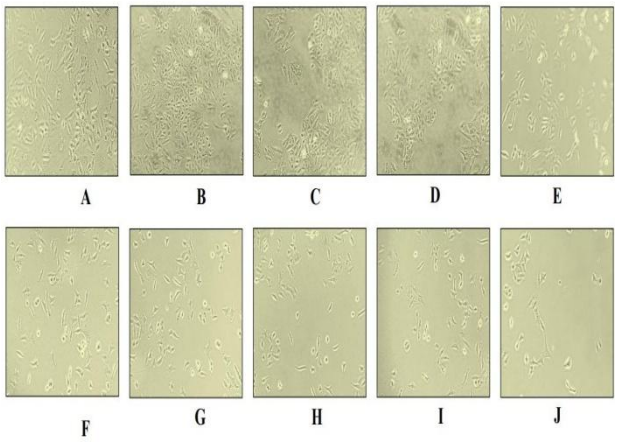

Figure 3. Dose–response curve showing the cytotoxic effect of the synthesized quinazoline derivative on A549 lung carcinoma cells (MTT assay).

The steep decline in cell viability with increasing concentrations suggests that 4-((1-(2- amino-6,7-dimethoxyquinazolin-4-yl)-1,4-dihydropyridin-3-yl)methyl)benzoicacideffectively interferes with mitochondrial metabolic activity, leading to cell death. Compared to the control group, treated cells showed pronounced morphological alterations such as rounding, detachment, and cell shrinkage, all of which are characteristic of apoptotic processes. The regression analysis (y=-13.84ln(x)+91.377)confirmedastronglogarithmicrelationship betweenconcentrationand cytotoxic response Table 1 . Further evaluation using acridine orange/ethidium bromide (AO/EtBr) dual staining revealedaprogressiveincreaseinapoptoticcellpopulationwithtime.After24hoursoftreatment, approximately 57% of the cells exhibited apoptotic morphology, which further increased to 66% after48hours.IllustratesonFigure4Thistime-dependentincreasehighlightsthat4-((1-(2-amino- 6,7-dimethoxyquinazolin-4-yl)-1,4-dihydropyridin-3-yl)methyl)benzoic acid triggers apoptosis rather than necrotic cell death.

Table1-logarithmic relationship between concentration and cytotoxic response

Concentration (µg/mL)	% Viability	Duplicate (%)	Triplicate (%)	MeanViability (%)	Standard Deviation
512	5.628	5.472	5.380	5.493	±0.125
256	16.021	15.540	15.632	15.731	±0.255
128	24.667	24.694	24.997	24.786	±0.183
64	32.502	32.870	32.518	32.630	±0.207
32	41.645	41.846	41.937	41.809	±0.149
16	52.260	52.038	52.022	52.106	±0.132
8	61.895	62.485	62.306	62.229	±0.302
4	72.023	72.888	73.267	72.726	±0.637
2	83.064	82.832	83.064	82.987	±0.134
1	91.137	91.440	91.802	91.460	±0.332

Collectively, the MTT and AO/EtBr analyses indicate that 4-((1-(2-amino-6,7- dimethoxyquinazolin-4-yl)-1,4-dihydropyridin-3-yl)methyl)benzoic acid possesses potent anticanceractivityagainstA549cellsbyinducingapoptosisina dose-andtime-dependentmanner. The relatively low IC_{50}value compared to other tested compounds supports its potential as a promising candidate for further mechanistic and therapeutic investigations

InsilicoStudies

The molecular docking and induced fit docking (IFD) studies revealed detailed insights into the specific residue interactions responsible for anchoring the ligand within the KRASG12C binding pocket. The ligand formed stabilizing hydrogen bonds and polar contacts primarily with Asp12, Gly13, and Gly60, which are known to be critical for recognition within the active site. Additional hydrophobic and π–π stacking interactions were observed with Val9, Thr58, Gln61, His95, Tyr96, and Ala85.

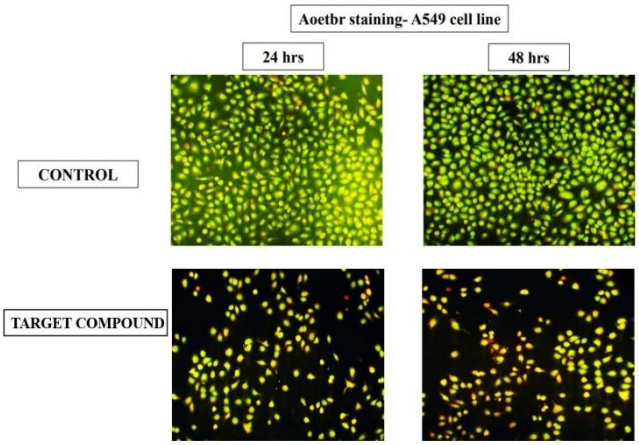

Figure 4.FluorescencemicroscopicimagesofAO/EtBr-stainedA549cellsafter24 and 48hours of compound treatment showing viable (green),early apoptotic (yellow/orange),and late apoptotic (red) c

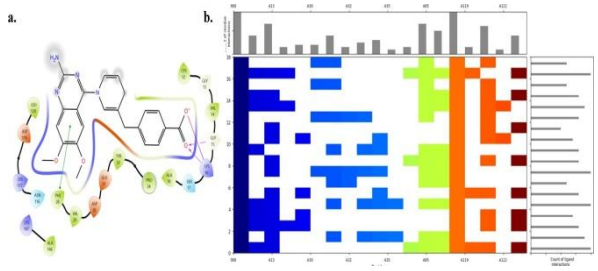

Figure 5 a. 2D interaction diagram of 4-((1-(2-amino-6,7-dimethoxyquinazolin-4-yl)-1,4- dihydropyridin-3-yl)methyl)benzoic acidand b,heatmap showing key KRASG12C residues involvedinligandbinding,highlightingfrequenthydrogen bondingandhydrophobicinteractions.

Notably,the interaction profile also involved residues such as Ala13,Ala30,Ala32,Ala35, Ala119, and Ala122, as confirmed by both the interaction diagram and contact heatmap. These interactions represent a combination of hydrogen bonds, van der Waals contacts, and aromatic stacking,collectivelycontributingtothestrongbindingenergy (MMGBSA−39.25kcal/mol)and docking score (−4.468) observed in computational studies. The spatial orientation of the ligand favors optimal engagement with both polar and apolar regions of the KRASG12C active site, supporting its candidacy for further optimization as a targeted inhibiton

CONCLUSION

The newly synthesized quinazoline derivative, 4-((1-(2-amino-6,7-dimethoxyquinazolin- 4-yl)-1,4-dihydropyridin-3-yl)methyl)benzoic acid, demonstrated potent cytotoxic and apoptotic effects against A549 human lung cancer cells. Structural confirmation through spectroscopic analyses validated the successful formation of the target compound.The MTTassay results established a clear dose-dependent reduction in cell viability, highlighting its significant antiproliferative potential. Furthermore, AO/EtBr dual staining analysis revealed that the compound promotes apoptosis in a time-dependent manner,suggesting that its anticancer activity is primarily mediated through apoptotic pathways rather than necrosis. The combination of synthetic feasibility, strong cytotoxic response and confirmed apoptotic induction under scores the pharmacological promise of this quinazoline scaffold. Future studies focusing on molecular docking, target interaction analysis, and in vivo evaluation are warranted to elucidate its mechanism of action and therapeutic applicability in NSCLC treatment

REFERENCE

1. Jaiswal S, Arya N, Yaduvanshi N, Devi M, Jain S, Jain S, Dwivedi J, Sharma S. Current updates on green synthesis and biological properties of 4-quinolone derivatives. Journal of Molecular Structure. 2023;1294. DOI:10.1016/j.molstruc.2023.
2. Ugwu DI, Okoro UC, Mishra NK. Synthesis, characterization and in vitro anti trypanosomal activities of new carboxamides bearing quinoline moiety. PLoS One. 2018;13:e0191234. DOI:10.1371/journal.pone.0191234
3. El-Kalyoubi S, El-Sebaey SA, Rashad AM, AL-Ghulikah HA, Ghorab MM, Elfeky SM. Synthesis, DFT calculations, and anti-proliferative evaluation of pyrimidine and selenadiazolopyrimidine derivatives as dual Topoisomerase II and HSP90 inhibitors. Journal of Enzyme Inhibition and Medicinal Chemistry. 2023;38. DOI:10.1080/14756366.2023.
4. Yang KH, Yen CY, Wang SC, Chang FR, Chang MY, Chan CK, Jeng JH, Tang JY, Chang HW. 6-n-Butoxy-10-nitro-12,13-dioxa-11-azatricyclo[73102,7]trideca-2,4,6,10-tetraene improves the X-ray sensitivity on inhibiting proliferation and promoting oxidative stress and apoptosis of oral cancer cells. Biomedicines. 2024;12:458. DOI:10.3390/biomedicines12020458
5. Mohammed Zaidh S, Aher KB, Bhavar GB, Irfan N, Ahmed HN, Ismail Y. Genes adaptability and NOL6 protein inhibition studies of fabricated flavan-3-ols lead skeleton intended to treat breast carcinoma. International Journal of Biological Macromolecules. 2023;127661. 258(Pt 1) DOI:10.1016/j.ijbiomac.2023.127661
6. Nobori T, Miura K, Wu DJ, Lois A, Takabayashi K, Carson DA. Deletions of the cyclin- dependent kinase-4 inhibitor gene in multiple human cancers. Nature. 1994;368:753–756. DOI:10.1038/368753a0
7. Braña MF, Cacho M, García ML, Mayoral EP, López B, De Pascual-Teresa B, Ramos A, Acero N, Llinares F, Muñoz-Mingarro D, Lozach O, Meijer L. Pyrazolo[3,4-c]pyridazines as novel and selective inhibitors of cyclin-dependent kinases. Journal of Medicinal Chemistry. 2005;48(21):6843–6854. DOI:10.1021/jm050486q

8. Yuan H, Liu Q, Zhang L, Hu S, Chen T, Li H, Chen Y, Xu Y, Lu T. Discovery, optimization and biological evaluation for novel c-Met kinase inhibitors. European Journal of Medicinal Chemistry. 2018;143:491–502. DOI:10.1016/j.ejmech.2017.11.051
9. Drexler HG, Matsuo Y, MacLeod RAF. Continuous hematopoietic cell lines as model systems for leukemia-lymphoma research. Leukemia Research. 2000;24(10):881–911. DOI:10.1016/S0145-2126(00)00103-4
10. Jin H, Zhang C, Zwahlen M, von Feilitzen K, Karlsson M, Shi M, Yuan M, Song X, Li X, Yang H, Turkez H, Fagerberg L, Uhlén M, Mardinoglu A. Systematic transcriptional analysis of human cell lines for gene expression landscape and tumor representation. Nature Communications. 2023;14:1–15.DOI:10.1038/s41467-023-39049-2
11. Calderón-Arancibia J, Espinosa-Bustos C, Cañete-Molina Á, Tapia R, Faúndez M, Torres M, Aguirre A, Paulino M, Salas C. Synthesis and pharmacophore modelling of 2,6,9-trisubstituted purine derivatives and their potential role as apoptosis-inducing agents in cancer cell lines. Molecules. 2015;20(4):6808–6826.DOI:10.3390/molecules20046808
12. Eser M, Hekimoglu G, Yarar MH, Canbek S, Ozcelik M. KRAS G12C mutation in NSCLC in a small genetic center: insights into sotorasib therapy response potential. Scientific Reports. 2024;14:26581.DOI:10.1038/s41598-024-66566-3
13. Emami L, Hassani M, Mardaneh P, Zare F, Saeedi M, Emami M, Khabnadideh S, Sadeghian S. 6-Bromo quinazoline derivatives as cytotoxic agents: design, synthesis, molecular docking and MD simulation. BMC Chemistry. 2024;18:125. DOI:10.1186/s13065-024-01113-2
14. Jagdale BS, Adole VA, Pawar TB, Desale BS. Molecular structure, frontier molecular orbitals, MESP and UV–Visible spectroscopy studies of ethyl 4-(3,4-dimethoxyphenyl)-6-methyl-2-oxo- 1,2,3,4-tetrahydropyrimidine-5-carboxylate: A theoretical and experimental appraisal. Material Science Research India. 2020;17(1):13–26. DOI:10.13005/msri/170102
15. Srinivasan M, Ismail Y, Irfan N, Mohammed Zaidh S. Synergistic suppression of cell growth: Phenmiazine derivatives targeting p53 and MDM2 unveiled through hybrid computational method. Computational Biology and Chemistry.2025;115:108344. DOI:10.1016/j.compbiolchem.2025.108344
16. Haja Nazeer Ahamed , Ismail Y , Irfan Navabshan [1], Mohammed Zaidh S , Shanmugarajan Ts , Ilham Jaleel , Thameemul Ansari Lh. Investigating the toxicity of malachite green and copper sulfate in brine shrimp: In-vivo and computational study. Toxicology Reports. 2024;13:101811. DOI:10.1016/j.toxrep.2024.101811
17. Zaidh SM, Vengateswaran HT, Habeeb M, Aher KB, Bhavar GB, Irfan N, Lakshmi KNVC. Network pharmacology and AI in cancer research uncovering biomarkers and therapeutic targets for RALGDS mutations. Scientific Reports. 2025;15:10938. DOI:10.1038/s41598-025-10938-7
18. Hussain H, Ahmad S, Abd Razak MF, Wan Mohamud WN, Bakar J, Mohd Ghazali H. Determination of cell viability using acridine orange/propidium iodide dual-spectrofluorometry assay. Cogent Food and Agriculture.2019;5:1582398. DOI:10.1080/23311932.2019.1582398
19. Irfan N, Vaithyanathan P, Anandaram H, Mohammed Zaidh S, Priya Varshini S, PuratchikodyA.Activeand allosteric site binding MM-QM studies of methylidene tetracyclo derivative in PCSK9 protein intended to make a safe antilipidemic agent. Journal of Biomolecular Structure and Dynamics. 2023.DOI:10.1080/07391102.2023.
20. Ramadan SK, Abd-Rabboh HSM, Abdel Hafez AA, Abou-Elmagd WSI. Some pyrimidohexahydroquinoline candidates: synthesis, DFT, cytotoxic activity evaluation, molecular docking, and in silico studies. RSC Advances. 2024;14:16584–16599. DOI:10.1039/D4RA01861K
21. Friesner RA, Banks JL, Murphy RB, Halgren TA, Klicic JJ, Mainz DT, Repasky MP, Knoll EH, Shelley M, Perry JK, Shaw DE, Francis P, Shenkin PS. Glide: A new approach for rapid, accurate docking and scoring. 1. Method and assessment of docking accuracy. Journal of Medicinal Chemistry. 2004;47(7):1739–1749. DOI:10.1021/jm0306430
22. Kitchen DB, Decornez H, Furr JR, Bajorath J. Docking and scoring in virtual screening for drug discovery: Methods and applications. Nature Reviews Drug Discovery. 2004;3(11):935–949. DOI:10.1038/nrd1549